

CleanCity IoT: A Vehicle-Mounted Platform for Real-Time Urban Air-Quality Monitoring and Forecasting in Resource-Constrained African Cities

Eric Nizeyimana¹, Damien Hanyurwimfura², Gabriel Uwanyirigira³,
Bonaventure Karikumutima⁴, Jimmy Nsenga⁵, Irene Niyonambaza Mihigo⁶

School of ICT, University of Rwanda, Kigali, Rwanda^{1, 2, 3, 4}

IT, 2Guiz SPRL, Brussels, Belgium⁵

School of ACEIoT, Rwanda Polytechnic, Kigali, Rwanda⁶
IT, Adventist University of Central Africa, Kigali, Rwanda¹

Abstract—Urban air pollution is a growing public-health challenge in African cities, yet traditional monitoring stations are sparse and expensive. The paper presents CleanCity IoT, a deployed, low-cost, vehicle-mounted air-quality platform that combines IoT sensors, GSM connectivity, cloud aggregation, and machine learning to produce near-real-time exposure maps and 2-hour forecasts for multiple pollutants. Each device integrates low-cost sensors for PM_{2.5}, PM₁₀, NO₂, O₃, SO₂, and CO₂, alongside temperature and humidity. Measurements are geotagged and transmitted over mobile networks from vehicles to a cloud backend, where data are validated, stored, and visualized through a user-friendly dashboard that also issues automated alerts and periodic reports. Using a dataset collected in Kigali and secondary cities via routine vehicular routes, the paper introduces the training of a multivariate time-series model to forecast short-horizon pollutant levels, supporting proactive health guidance and regulatory action. The system reports a performance in terms of latency, uptime, coverage, and data quality, and evaluate forecast accuracy using MAE/RMSE/MAPE and event-oriented metrics for spike prediction. Results indicate that CleanCity IoT provides reliable, scalable, and cost-effective urban air-quality intelligence, closing key gaps in spatiotemporal coverage while enabling citizen access, policy support, and social impact. The platform demonstrates a practical blueprint for African cities to operationalize air-quality intelligence using existing mobile infrastructure and locally developed technology.

Keywords—CleanCity IoT; air quality; mobile sensing; multivariate forecasting; spike detection

I. INTRODUCTION

Urban air pollution has emerged as one of the fastest-growing environmental and public-health threats in African cities such as Kigali, Rwanda, driven by rapid urbanization, motorization, and industrial expansion [1][2]. The World Health Organization (WHO) reports that air pollution causes over seven million premature deaths annually, while nearly 90% of the global population is exposed to pollutant concentrations exceeding recommended limits. In many low- and middle-income countries, fine particulate matter (PM_{2.5} and PM₁₀) and gaseous pollutants such as nitrogen dioxide (NO₂), sulfur

This work was supported by a generous grant from PASET/RSIF, without whom this project would not have been possible.

dioxide (SO₂), ozone (O₃), and carbon dioxide (CO₂) remain poorly monitored, limiting the capacity for evidence-based policymaking and citizen awareness [3]. Recent environmental assessments in Kigali have revealed that PM_{2.5} concentrations during peak hours often surpass 50 $\mu\text{g}/\text{m}^3$, nearly double the WHO 24-hour guideline, highlighting an urgent need for high-resolution, real-time monitoring systems [4].

Conventional air-quality monitoring infrastructures, which depend on fixed high-precision stations, provide accurate but spatially limited data. Their high installation and maintenance costs prevent widespread deployment across large or topographically diverse urban areas. Consequently, most African cities rely on sparse or intermittent measurements that fail to capture micro-scale variations and short-term pollution spikes. In response, researchers have turned to low-cost Internet of Things (IoT)-based sensing networks that offer dense, distributed data acquisition at a fraction of the traditional cost [4], [5]. Among the most effective configurations are vehicle-mounted sensor systems, which leverage the mobility of public-service vehicles, taxis, and buses to achieve city-wide spatial coverage without constructing new fixed stations [5] [6] [7].

Earlier studies such as [8] on affordable vehicle-mounted monitoring, [9] on IoT devices for municipal vehicles, and [6] on bus-based monitoring platforms have demonstrated the technical feasibility of mobile air-quality mapping and visualization. These systems collect particulate and gaseous pollutants while traversing city corridors, producing near-real-time datasets for spatial pattern analysis. However, most prior implementations primarily focused on measurement and visualization, offering limited integration of predictive analytics, alert systems, and policy-support mechanisms—features crucial for proactive environmental management, especially in data-scarce regions.

Building upon these efforts, this study introduces CleanCity IoT, a low-cost, scalable, and mobile air-quality monitoring and forecasting platform developed at the University of Rwanda in collaboration with national and regional partners. Each CleanCity IoT unit integrates low-cost sensors for PM_{2.5}, PM₁₀, NO₂, SO₂, O₃, and CO₂, along with temperature and humidity modules, controlled by an ESP32 microcontroller equipped with

GSM connectivity. The devices are mounted on moving vehicles, enabling spatially continuous air-quality sampling across Kigali and secondary cities. Data are transmitted via mobile networks to a cloud server (ThingSpeak), where they are cleaned, stored, and visualized through a real-time web dashboard featuring pollution heat maps, alert notifications, and automated reporting tools. Fig. 1 illustrates the overall CleanCity IoT ecosystem, including its sensing, communication, and analytics layers.

A distinctive feature of CleanCity IoT is the inclusion of a machine-learning forecasting module that predicts pollutant levels up to two hours ahead based on multivariate time-series data. This capability enables early warnings and supports informed interventions by environmental authorities, health agencies, and city planners. Furthermore, by making air-quality information publicly accessible through a user-friendly dashboard, the system strengthens community engagement and promotes citizen science, aligning with Rwanda's Smart-City and environmental-sustainability initiatives.

The proposed study builds upon the foundational work by [10], [11], who developed an IoT-edge-based prototype for detecting transportation-related pollution spikes in Kigali. Their system demonstrated the feasibility of using low-cost IoT networks for real-time air-quality monitoring in urban transport corridors. However, while the earlier prototype focused primarily on localized pollution detection and data transmission through edge networks, the present research extends this framework into a fully integrated CleanCity IoT system that includes mobile GSM-based data collection, cloud dashboard visualization, and machine-learning-driven forecasting. Thus, this study represents both continuation and enhancement of the ACEIoT initiative's earlier work, translating edge-level monitoring into a scalable, citizen-centered solution for smart urban management.

A. Contributions

The key contributions of this work are as follows:

- Design and deployment of a vehicle-mounted IoT device integrating multi-pollutant gas and particulate sensors with GSM-based real-time communication.
- Implementation of a cloud-hosted dashboard providing visualization, alerting, and reporting functionalities for stakeholders.
- Development of a multivariate machine-learning model for two-hour-ahead pollutant prediction, supporting proactive urban-health responses.
- Field validation of the system in Kigali and secondary cities, demonstrating low-cost scalability, data reliability, and practical usability.
- Promotion of local innovation and social impact, reinforcing Rwanda's vision for smart and sustainable urban management.

Through these contributions, CleanCity IoT establishes a practical, home-grown framework for real-time, predictive, and socially inclusive air-quality intelligence applicable to cities across Africa.

B. Paper Organization

The remainder of this paper is structured as follows: Section II reviews related work on mobile air-quality sensing and forecasting techniques. Section III describes the system design, algorithm construction and hardware implementation. Section IV presents data-processing and machine-learning methodologies. Section V discusses experimental results and performance evaluation, and Section VI concludes with key findings and future research directions.

II. RELATED WORK

A. Conventional and Fixed-Station Monitoring

Traditional air-quality surveillance depends on reference-grade analyzers that provide highly accurate but spatially limited data. These stations, typically operated by environmental agencies, can cost more than USD 50,000 per unit, with significant yearly maintenance expenses [8]. Such systems monitor only a few fixed locations, resulting in low spatial coverage that fails to capture localized variations in pollutants caused by traffic density, topography, or industrial activities. While essential for calibration and regulatory baselines, fixed networks are financially unsustainable for widespread deployment in developing countries.

B. Emergence of Low-Cost IoT Sensor Networks

Advances in sensor miniaturization, embedded microcontrollers, and cloud connectivity have led to low-cost IoT-based monitoring systems [12], [13]. These frameworks employ microcontrollers such as Arduino or ESP32 and communication technologies including Wi-Fi, GSM, or LoRa to transmit environmental data in real time. Gubbi *et al.* (2013) outlined a scalable IoT architecture for smart environments that has since inspired numerous urban-sensing deployments. Although low-cost sensors are less accurate than reference analyzers, they enable dense spatial coverage, data fusion, and temporal tracking when coupled with calibration algorithms or machine learning [5], [14].

C. Mobile and Vehicle-Mounted Sensing Approaches

To improve spatial resolution, several researchers have adopted mobile sensing using vehicles as carriers. The paper [12] designed an affordable vehicle-mounted system for dynamic air-quality mapping. In the papers [6] implemented a bus-based monitoring platform integrated with cloud dashboards for real-time visualization. The paper [9] deployed IoT modules on municipally governed vehicles to track NO₂ and particulate matter across city zones. The paper in [7] proposed a vehicular sensor network architecture for real-time pollution analysis, while the paper [15] validated low-cost mobile sensors for hyperlocal monitoring in London. These projects proved the feasibility of vehicular IoT systems, but most emphasized data collection and visualization, with limited inclusion of predictive analytics, alerts, or decision-support tools.

A recent Rwandan contribution in the paper [10] introduced an IoT-edge-based system for detecting transportation pollution spikes using embedded edge computing. Their implementation at the Africa Centre of Excellence in Internet of Things (ACEIoT) validated the use of localized edge devices for

vehicular pollution tracking. Building on this foundation, the current CleanCity IoT framework enhances mobility, scalability, and predictive intelligence through GSM-based data transmission and cloud-integrated analytics.

D. Cloud-Based Data Aggregation and Visualization

Cloud computing has become central to IoT ecosystems for environmental data management. Platforms such as ThingSpeak, AWS IoT Core, and Azure IoT Hub support data ingestion, storage, and visualization in real time [1], [6], [13], [14], [16], [17]. The papers [2], [18] [6] demonstrated city-wide dashboards for pollutant tracking, and [7] discussed open-source architectures for mobile-data integration with geographic information systems. Nevertheless, most cloud-based implementations stop at visualization, lacking automated alerting, policy analytics, and citizen-accessible interfaces key enablers for social impact.

E. Machine-Learning Forecasting for Air Quality

Accurate short-term forecasting of air pollutants enables preventive interventions. Statistical models such as ARIMA and VAR have been widely used for one-step-ahead predictions, but deep-learning approaches now dominate multivariate time-series forecasting [19]. LSTM and GRU networks, as explored in paper [20] outperform linear models in capturing nonlinear temporal dependencies of PM_{2.5} and NO₂ concentrations. Despite these advances, few studies integrate such predictive analytics directly into mobile, low-cost IoT frameworks, particularly within African contexts where both connectivity and calibration data are limited.

Quantitatively, low-cost sensor units in these studies ranged from USD 150–300 per node, achieved spatial resolutions up to

100m, and showed mean deviations of $\pm 10\text{--}20\%$ compared with reference instruments [6], [7], [12]. Such performance is adequate for mapping and trend detection but insufficient for health-critical forecasting without data calibration and model correction.

F. Research Gap and Motivation

Despite the progress summarized above, major limitations persist:

- Lack of integrated forecasting and alerting modules within mobile IoT systems.
- Absence of region-specific deployments in sub-Saharan Africa using GSM infrastructure for scalable connectivity.
- Minimal incorporation of citizen-accessible dashboards and community engagement mechanisms.

The CleanCity IoT platform directly addresses these challenges by combining multi-pollutant IoT sensing, GSM data transmission, cloud-based visualization, and machine-learning-driven forecasting. The project exemplifies a locally developed, cost-effective solution advancing both environmental intelligence and social awareness.

The reviewed literature highlights a steady evolution from fixed-station monitoring toward IoT-enabled, mobile, and data-driven frameworks as shown in Table I. However, none fully integrate predictive analytics, social accessibility, and regional scalability within a single platform. Section III therefore presents the system design and implementation of the proposed CleanCity IoT solution, detailing its hardware architecture, communication model, and cloud-analytics workflow.

TABLE I. COMPARATIVE SUMMARY OF RELATED IOT AND MOBILE AIR-QUALITY MONITORING SYSTEMS

Author & Year	Platform System	Methodology Features	Key Contribution	Identified Limitation
Santana et al. (2021)	Vehicle-mounted AQ mapping	ESP32 + GSM; PM _{2.5} / NO ₂ sensing	Affordable mobile monitoring	No predictive analytics
Ivanova et al. (2020)	IoT on municipal vehicles	Wi-Fi IoT nodes; CO PM sensors	Dynamic city-wide mapping	Limited citizen interface
Correia et al. (2023)	Bus-based AQ system	Cloud dashboard visualization	Real-time city dashboards	No forecasting capability
Zherka & Tafa (2023)	Vehicular sensor network	On-board sensors + data fusion	Real-time analysis	Lacks scalability
Zboralski & Kunz (2024)	Mobile GIS framework	Cloud integration	Open-source architecture	No alert or policy module
CleanCity IoT (this work)	Vehicle IoT + GSM + ML	ESP32 + GSM + ThingSpeak + LSTM	Real-time forecasting + dashboard + alerts	-----

III. METHODOLOGY

A. Overview of the Proposed Framework

The CleanCity IoT framework is designed as an end-to-end intelligent air-quality monitoring and forecasting system that leverages Internet of Things (IoT), cloud computing, and machine learning (ML) technologies to provide real-time insights into urban pollution dynamics. The framework aims to transform conventional monitoring often limited to fixed stations into a mobile, scalable, and predictive sensing ecosystem suited for low-resource contexts such as Rwandan cities.

In Fig. 1, the system operates through four tightly integrated layers: 1) sensing and acquisition, 2) communication and

transmission, 3) cloud storage and analytics, and 4) visualization and forecasting. Each layer contributes specific functionalities, forming a pipeline that converts raw sensor readings into actionable intelligence for environmental management and policy decision-making.

In the sensing and acquisition layer, a suite of low-cost environmental sensors continuously measures air pollutants including particulate matter (PM_{2.5}, PM₁₀), nitrogen dioxide (NO₂), sulfur dioxide (SO₂), ozone (O₃), and carbon dioxide (CO₂), alongside ambient parameters such as temperature and humidity. These sensors are interfaced with an ESP32 microcontroller integrated with a SIM800L GSM module, enabling both data collection and mobile transmission from vehicle-mounted units.

The communication and transmission layer employs GSM/GPRS connectivity for real-time data delivery to cloud infrastructure. This design choice compared to Wi-Fi or LoRa is motivated by the wide availability of mobile networks across Rwandan cities and highways, ensuring scalability and mobility without dependency on fixed infrastructure.

The cloud layer utilizes the ThingSpeak IoT platform, which serves as both a data repository and preliminary analytics engine. Each sensing node transmits periodic measurements (every 30 seconds to 1 minute) to predefined ThingSpeak channels through HTTP POST requests. The platform aggregates, timestamps, and visualizes incoming data streams, while also allowing external APIs for integration with advanced analytical tools such as MATLAB, Python, or Node-RED for extended processing and forecasting.

The visualization and forecasting layer bridge the system's technical outputs with end-user interaction. A custom Air Quality Dashboard accessible via web or mobile interface—displays real-time pollutant levels, temporal trends, and geospatial mapping of emission zones. Historical datasets retrieved from ThingSpeak are used to train a Long Short-Term Memory (LSTM)-based predictive model, which forecasts pollutant concentrations two hours ahead. This predictive feature enhances early-warning capabilities and supports data-driven policy interventions by environmental authorities.

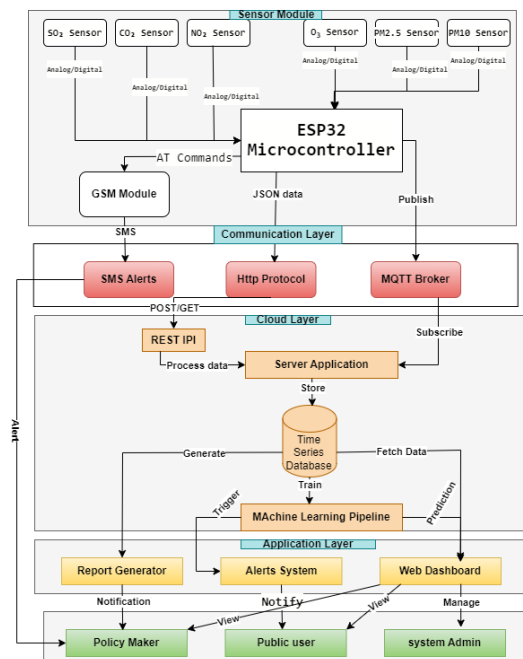


Fig. 1. Proposed framework.

B. Hardware Design and Components

The CleanCity IoT hardware architecture was designed to achieve low-cost, high-mobility, and energy-efficient air-quality monitoring while maintaining compatibility with existing mobile communication networks. The system integrates multiple sensors, a microcontroller unit, and a GSM communication interface, all mounted within a compact enclosure suitable for vehicular deployment.

1) *Main controller: ESP32 (LilyGO T-Call SIM800L)*: At the core of the system lies the LilyGO T-Call ESP32 board on Fig. 2, which combines a dual-core 32-bit Xtensa processor with an embedded SIM800L GSM/GPRS module. The ESP32 manages sensor data acquisition, preprocessing, and transmission, while the GSM modem handles real-time communication with the cloud platform. The built-in UART, ADC, and GPIO interfaces facilitate multi-sensor connectivity, and the board supports 3.3 V logic with a stable 5 V input via USB or Li-ion battery.

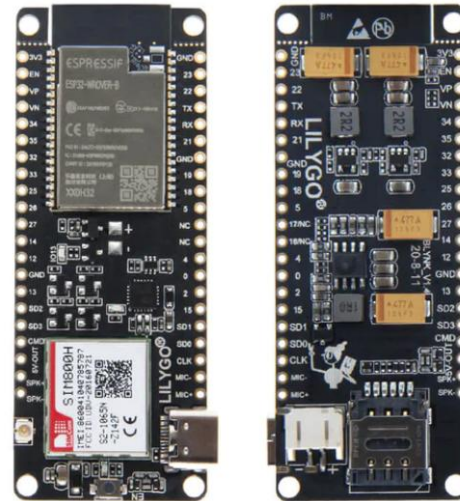


Fig. 2. LilyGO T-Call SIM800L.

The SIM800L module provides reliable 2G cellular connectivity, using HTTP POST requests to upload sensor readings to ThingSpeak channels. The use of GSM ensures that each node remains fully mobile and independent of Wi-Fi coverage, a critical feature for vehicle-mounted monitoring units in Rwandan cities and peri-urban areas.

2) *Sensor suite*: The CleanCity IoT system employs a diverse set of environmental sensors to capture the most relevant atmospheric parameters affecting air quality. Each sensor was selected for its low cost, stability, and proven performance in mobile IoT applications.

3) *PMS5003 – particulate matter (PM_{2.5} and PM₁₀)*: The Plantower PMS5003 in Fig. 3 is a laser-scattering particulate matter sensor capable of measuring fine and coarse particles (PM_{2.5} and PM₁₀) in real time. It uses a light-scattering principle combined with a digital signal processor to calculate mass concentration in micrograms per cubic meter ($\mu\text{g}/\text{m}^3$). The sensor communicates via UART and offers high sensitivity and accuracy suitable for vehicular environments, making it ideal for continuous mobile air-quality monitoring.

4) *MQ-131 – Ozone (O₃) sensor*: The MQ-131 sensor in Fig. 4 detects ozone concentrations using a tin dioxide (SnO₂)-based semiconductor layer. When O₃ gas contacts the sensitive surface, it alters the material's conductivity proportionally to the gas concentration. The analog output from the sensor is fed to the ESP32's ADC pin, which converts it into a corresponding O₃ level in parts per million (ppm). This sensor was chosen for

its low cost and reasonable response time, essential for detecting short-term pollution spikes.

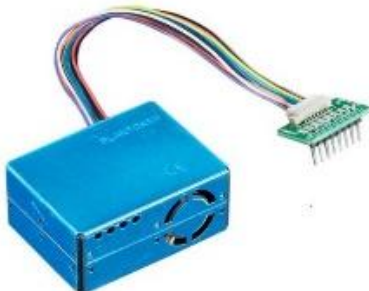


Fig. 3. Plantower PMS5003.



Fig. 4. MQ-131 sensor.

5) *MICS-6814 – Nitrogen Dioxide (NO₂) Sensor*: The MICS-6814 in Fig. 5 is a compact three-channel semiconductor gas sensor that simultaneously measures NO₂, CO, and NH₃ gases. It is particularly suitable for mobile IoT applications due to its low power consumption and small form factor. For this project, the NO₂ channel was primarily used, with calibration coefficients adjusted based on the manufacturer's characterization curve. Its analog signal provides ppm-level readings processed by the ESP32's 12-bit ADC.



Fig. 5. Nitrogen Dioxide (NO₂) sensor.

6) *AGSM-SO₂-5 Sulfur Dioxide (SO₂) sensor*: The AGSM-SO₂-5 in Fig. 6 is an electrochemical-type sensor used to detect sulfur dioxide concentrations in ambient air. The sensor produces a small current proportional to the SO₂ gas concentration, which is converted to voltage using an external resistor circuit and read through an ADC input. This sensor type offers high selectivity and low detection limits, enabling reliable SO₂ measurement even in mixed-gas environments. Its readings are periodically calibrated against baseline voltages under clean-air conditions.

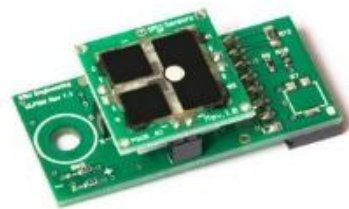


Fig. 6. Sulfur Dioxide (SO₂) sensor.

7) *MG-811 Carbon Dioxide (CO₂) sensor*: The MG-811 sensor in Fig. 7 measures carbon dioxide (CO₂) concentration using a solid electrolyte cell. The sensor outputs an analog voltage that decreases as CO₂ concentration increases. It operates between 0–10,000 ppm and provides stable performance for mobile applications when coupled with proper temperature compensation. The MG-811 data complements the other gas readings by offering insights into combustion-related emissions.



Fig. 7. Carbon Dioxide (CO₂) sensor.

8) *DHT11 temperature and humidity sensor*: The DHT11 digital sensor in Fig. 8 monitors ambient temperature and relative humidity, parameters that directly influence gas sensor accuracy and pollutant dispersion. Its single-wire digital output simplifies integration with the ESP32 microcontroller. The temperature and humidity data collected are used to normalize and interpret gas readings, reducing variability due to environmental factors.

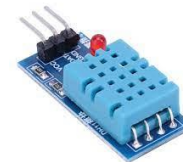


Fig. 8. DHT11 temperature and humidity sensor.

C. Custom PCB Design and Circuit Integration

To ensure a compact, reliable, and vibration-resistant mobile sensing unit, the system incorporates a custom-designed PCB, created using EasyEDA and manufactured as a single-layer board. The PCB consolidates all key components including the LilyGO T-Call ESP32, PMS5003 particulate matter sensor, MQ131 ozone module, CJMCU-6814 multi-gas sensor (NO₂ +

SO_2), and analog SO_2 sensor interface into a unified hardware platform optimized for vehicular deployment.

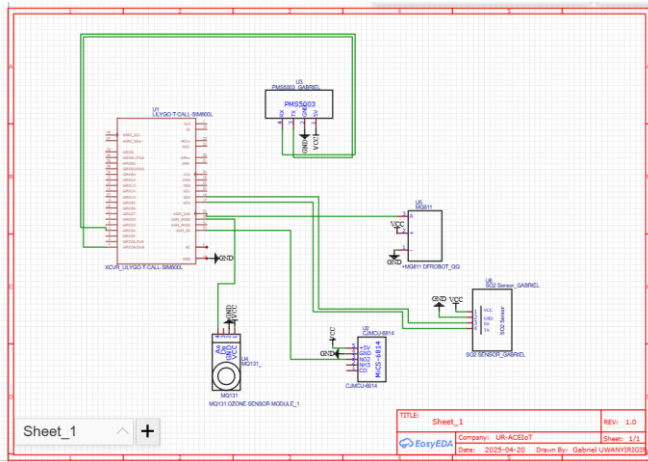


Fig. 9. Schematic diagram of clean city IoT system.

The PCB layout in Fig. 9 follows a structured placement strategy, with the PMS5003 connector positioned on the upper-left side to minimize trace length for the UART interface, while the MQ131 and CJMCU-6814 modules are placed on the right to avoid electromagnetic interference from the GSM modem. Dedicated headers provide labeled terminals for VCC, GND, RX, and TX, ensuring clear wiring during assembly and simplifying sensor maintenance or replacement. The bottom section houses the footprint for the LilyGO T-Call board, providing direct access to GSM, UART, and ADC lines without intermediate wiring.

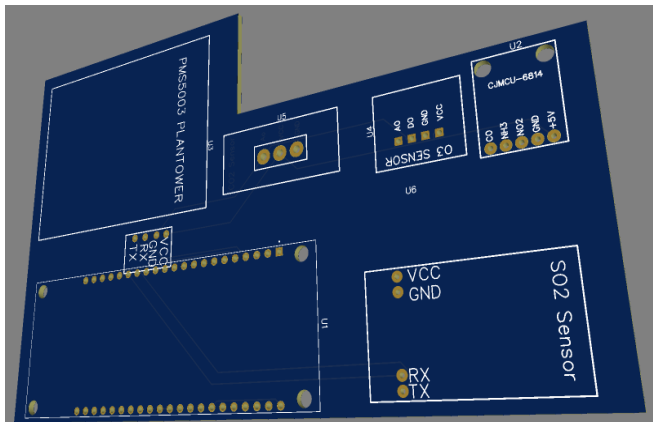


Fig. 10. 3D view of the custom PCB design for the CleanCity IoT device.

The corresponding circuit schematic (Fig. 10) illustrates the electrical interconnections between all sensing modules and the ESP32 controller. UART pins are assigned to the PMS5003 (U3) and SO_2 sensor interface, while the MQ131 analog output is routed to an ADC input. The CJMCU-6814 module is powered by a stable 5V rail, and its NO_2/SO_2 analog channels are fed into separate ADC lines for accurate digital conversion. Ground planes and decoupling capacitors are incorporated to enhance signal stability and reduce noise, which is critical for gas sensor accuracy. The PCB also accommodates optional onboard filtering capacitors for the analog channels, further increasing measurement reliability.

This custom PCB significantly enhances the robustness of the CleanCity IoT device compared to breadboard-based prototypes. By minimizing loose wiring, standardizing sensor interfaces, and optimizing component placement, the board improves electrical reliability, reduces interference from the GSM module, and ensures consistent sensor readings during mobile operation. It also enables rapid replication of the device for larger-scale deployments in Kigali or other Rwandan cities.

D. Data Acquisition and Transmission

The CleanCity IoT system collects, processes, and transmits multi-sensor environmental data in real time through a unified acquisition pipeline. The design ensures synchronized sampling across all sensing modules, reliable communication via GSM, and consistent data formatting for cloud integration.

E. Sensor Data Acquisition Cycle

Each monitoring node performs periodic measurements of particulate matter, gaseous pollutants, and ambient conditions.

- **Particulate Matter ($\text{PM}_{2.5}$ and PM_{10}):** The PMS5003 sensor provides continuous data through a UART interface, reporting particle concentrations in $\mu\text{g}/\text{m}^3$.
- **Gaseous Pollutants: O_3 , NO_2 , SO_2 , and CO_2 :** Levels are sensed using analog sensors (MQ-131, MICS-6814, AGSM- SO_2 -5, and MG-811). Their analog voltages are sampled by the ESP32's 12-bit ADC and converted to concentration values (ppm) using calibration curves derived from reference data.
- **Ambient Conditions:** The DHT11 sensor provides temperature and relative-humidity readings, which are used for contextual adjustment of gas-sensor responses.

To reduce random noise and ensure stability, multiple readings are averaged within each cycle before transmission. The resulting dataset per interval includes parameters as shown in Table II.

TABLE II. PARAMETERS ACQUIRED DURING EACH SAMPLING CYCLE

Parameter	Symbol	Unit
$\text{PM}_{2.5}$ concentration	$\text{PM}_{2.5}$	$\mu\text{g}/\text{m}^3$
PM_{10} concentration	PM_{10}	$\mu\text{g}/\text{m}^3$
Ozone	O_3	ppm
Nitrogen Dioxide	NO_2	ppm
Sulfur Dioxide	SO_2	ppm
Carbon Dioxide	CO_2	ppm
Temperature	T	$^{\circ}\text{C}$
Humidity	H	%

F. Data Pre-Processing and Packet Formation

Before transmission, each sensor reading undergoes a lightweight pre-processing pipeline to improve data reliability and ensure consistency across the full dataset. First, a noise-filtering procedure is applied to remove spurious or invalid sensor values. Given a raw reading x_i for pollutant j , the system checks whether it falls within the predefined operational range $[L_j, U_j]$. This filtering step is mathematically expressed as:

$$x'_i = \begin{cases} x_i & \text{if } L_j \leq x_i \leq U_j \\ \text{NaN} & \text{otherwise} \end{cases} \quad (1)$$

Ensuring that negative values, extreme spikes, and sensor glitches do not propagate into the cloud dataset.

Following outlier removal, each pollutant value is normalized into standard physical units ($\mu\text{g}/\text{m}^3$ or ppm) using a linear scaling transformation. This normalization converts raw sensor outputs into a consistent range defined by calibration limits, allowing accurate comparison across sensors. The conversion is achieved using Eq. (2).

$$x_{norm} = \frac{x_i - x_{min}}{x_{max} - x_{min}} \times (S_{max} - S_{min}) + S_{min} \quad (2)$$

where x_{max} and x_{min} are the sensor's calibrated electrical bounds and S_{max} , S_{min} correspond to the standardized environmental scale. This operation ensures homogeneous units throughout the dataset, which is essential for downstream analytics.

Each sanitized and normalized reading is then assigned a timestamp to preserve temporal integrity. The timestamp t_k originates either from the GSM network clock or the ESP32's internal real-time counter. The final structured data packet transmitted at time k is represented as,

$$D_k = \{DeviceID, PM_{2.5}, PM_{10}, O_3, NO_2, SO_2, CO_2, T, H, t_k\} \quad (3)$$

capturing all pollutants, environmental conditions, and metadata in a single, machine-readable structure compatible with ThingSpeak's REST API.

G. GSM-Based Data Transmission

The LilyGO T-Call ESP32 integrates a SIM800L GSM/GPRS modem, allowing each mobile sensing unit to transmit air-quality data directly to the cloud without requiring Wi-Fi or external gateways. Once a complete measurement vector

$$z_t = [PM_{2.5}, PM_{10}, O_3, NO_2, SO_2, CO_2, T, H] \quad (4)$$

is pre-processed, the system encapsulates the data into a structured transmission packet. The full packet sent at time t is expressed as:

$$P_t = \{DeviceID, z_t, t\} \quad (5)$$

Every transmission cycle follows a periodic schedule, where the upload interval is defined as

$$\Delta t = t_k - t_{k-1} \quad (6)$$

and during the experimental deployment, $\Delta t \approx 30$ s, providing a balance between data granularity and power efficiency for vehicular operation. The SIM800L modem performs an HTTP POST request over GPRS, where the payload corresponds to the encoded packet P_t . The uplink transmission can be represented as

$$\mathcal{T}(P_t) \rightarrow \text{ThingSpeak Channel} \quad (7)$$

where $\mathcal{T}(P_t)$ denotes the GSM-based upload operation. Once the server acknowledges receipt, ThingSpeak updates the real-time charts for all monitored pollutants. To ensure time-

series completeness, the system incorporates a local retransmission buffer. If a temporary network outage occurs, packets are stored in a local queue

$$\mathcal{Q} = \{P_{t_1}, P_{t_2}, \dots, P_{t_m}\} \quad (8)$$

and are automatically resent once connectivity is restored. Successful transmission empties the queue according to

$$\mathcal{Q} \leftarrow \mathcal{Q} \setminus P_{t_i} \quad (9)$$

This queue-based recovery mechanism guarantees robustness in urban mobility conditions, where cellular coverage may momentarily fluctuate. As a result, the system achieves reliable, timestamped uploads essential for downstream analytics, ML model training, and spatiotemporal pollution mapping.

H. Cloud Integration and Dashboard Development

The CleanCity IoT system relies on ThingSpeak Cloud as the central platform for ingesting, storing, and visualizing sensor data in real time. Each monitoring node continuously uploads the structured packet P_t to a dedicated ThingSpeak channel, where the information is automatically timestamped and organized across eight data fields. The cloud interface provides dashboards, charts, and API endpoints that support both manual inspection and automated analytical tasks such as forecasting and multi-pollutant correlation studies.

To quantify the data-handling performance of the cloud layer, the expected number of uploaded records over an observation period T is expressed as,

$$N_T = \frac{T}{\Delta t} \quad (10)$$

where, Δt represents the transmission interval (approximately 30 seconds in this deployment). This relation determines the temporal granularity and the total volume of data streamed into the cloud. The corresponding data throughput, crucial for evaluating network and storage efficiency, is computed using

$$R_{up} = \frac{N_T \times P_k}{T} \quad (11)$$

where, P_k denotes the average packet size in bytes. These metrics confirm that the system maintains consistent upload behavior, even under mobile conditions. In ThingSpeak, pollutant concentrations are further processed to compute an Air Quality Index (AQI). For each pollutant i , the platform evaluates a sub-index using

$$I_i = \frac{I_{high} - I_{low}}{C_{high} - C_{low}} (C_i - C_{low}) + I_{low} \quad (12)$$

where the constants correspond to standard AQI breakpoints.

The overall AQI at time t is determined by,

$$AQI = \max(I_i) \quad (13)$$

allowing the system to categorize air quality levels and support early-warning notifications when thresholds are exceeded.

The cloud platform also enables multi-variable diagnostic analysis, particularly through pollutant correlation. The linear

relationship between any two-pollutant series x_i and x_j is computed using the Pearson coefficient,

$$r_{ij} = \frac{\sum_{k=1}^n (x_{i,k} - \bar{x}_i)(x_{j,k} - \bar{x}_j)}{\sqrt{\sum_{k=1}^n (x_{i,k} - \bar{x}_i)^2} \sqrt{\sum_{k=1}^n (x_{j,k} - \bar{x}_j)^2}} \quad (14)$$

This allows identification of pollutant sources with similar temporal behaviors, such as $\text{PM}_{2.5}$ and NO_2 often linked to traffic emissions. To ensure reliability, ThingSpeak computes a data completeness index over any period T as,

$$C_T = \frac{N_s}{N_t} \times 100 \% \quad (15)$$

where N_s and N_t are the numbers of successfully uploaded and total expected packets, respectively. This metric is essential for confirming the robustness of GSM-based data acquisition, especially in mobile environments where connectivity might fluctuate. Through this cloud architecture, CleanCity IoT achieves real-time visualization, long-term storage, and automated analytic capability, making it suitable for continuous urban air-quality monitoring and predictive modeling.

I. Machine Learning Model Development

The dataset collected from the ThingSpeak cloud was used to train a Long Short-Term Memory (LSTM) neural network for short-term air-quality forecasting. The choice of LSTM was motivated by its ability to capture nonlinear temporal dependencies in multivariate time-series data, making it suitable for predicting pollutant levels under changing meteorological and traffic conditions. To prepare the data, each environmental variable was standardized to ensure consistent scaling across all pollutants. This normalization follows the transformation.

$$\hat{z}_t^{(i)} = \frac{z_t^{(i)} - \mu_i}{\sigma_i} \quad (16)$$

where, $\hat{z}_t^{(i)}$ denotes the original reading of feature i at time t , and μ_i and σ_i represent the corresponding mean and standard deviation. A sliding window of length L was then used to construct input sequences for the model. Each multivariate input window is defined as,

$$X_t = [\tilde{z}_{t-L+1}, \tilde{z}_{t-L+2}, \dots, \tilde{z}_t] \in R^{L \times 8} \quad (17)$$

while the prediction target for horizon H is given by,

$$y_t = z_{t+H} \quad (18)$$

The LSTM learns a nonlinear mapping

$$\hat{y}_t = f_\theta(X_t) \quad (18)$$

where, f_θ denotes the trained neural-network function parameterized by θ . The training objective is to minimize the Mean Squared Error (MSE):

$$\text{LMSE}(\theta) = \frac{1}{N} \sum_{t=1}^N \|y_t - \hat{y}_t\|_2^2 \quad (19)$$

Model performance was evaluated using Mean Absolute Error (MAE), Root Mean Square Error (RMSE), Mean Absolute Percentage Error (MAPE), and the coefficient of determination R^2 , expressed respectively as

$$MAE_j = \frac{1}{N} \sum_{t=1}^N |y_t^{(j)} - \hat{y}_t^{(j)}| \quad (20)$$

$$RMSE_j = \sqrt{\frac{1}{N} \sum_{t=1}^N (y_t^{(j)} - \hat{y}_t^{(j)})^2} \quad (21)$$

$$MAPE_j = \frac{100}{N} \sum_{t=1}^N \left| \frac{y_t^{(j)} - \hat{y}_t^{(j)}}{y_t^{(j)}} \right| \quad (22)$$

$$R_j^2 = 1 - \frac{\sum_{t=1}^N (y_t^{(j)} - \hat{y}_t^{(j)})^2}{\sum_{t=1}^N (y_t^{(j)} - \bar{y}^{(j)})^2} \quad (23)$$

These performance indicators assess the reliability of the LSTM model in forecasting pollutant levels such as $\text{PM}_{2.5}$, PM_{10} , NO_2 , SO_2 , O_3 , CO_2 , temperature, and humidity. By using standardized inputs and multivariate temporal windows, the model is able to produce stable forecasts up to two hours ahead, enabling early-warning capabilities and supporting real-time decision-making for environmental monitoring.

IV. RESULTS AND DISCUSSION

A. Dataset Characteristics

The CleanCity IoT mobile sensing unit collected a total of 6,484 multivariate records during vehicular movement across urban road segments in Kigali. Each record contains synchronized measurements of particulate pollution ($\text{PM}_{2.5}$, PM_{10}), gaseous pollutants (NO_2 , SO_2 , O_3 , CO_2), and meteorological variables (temperature and relative humidity). Data were transmitted at an average 30-second sampling interval, resulting in a dense and continuous time-series suitable for both statistical analysis and machine learning-based forecasting.

The temporal behavior of the dataset is illustrated in Fig. 11, which shows the evolution of $\text{PM}_{2.5}$, PM_{10} , NO_2 , and temperature over several days. The plots reveal clear short-term fluctuations driven by traffic movement, road dust resuspension, and localized emission hotspots commonly encountered during mobile sensing. The temperature curve exhibits a pronounced diurnal cycle, confirming environmental consistency and stable sensor response.

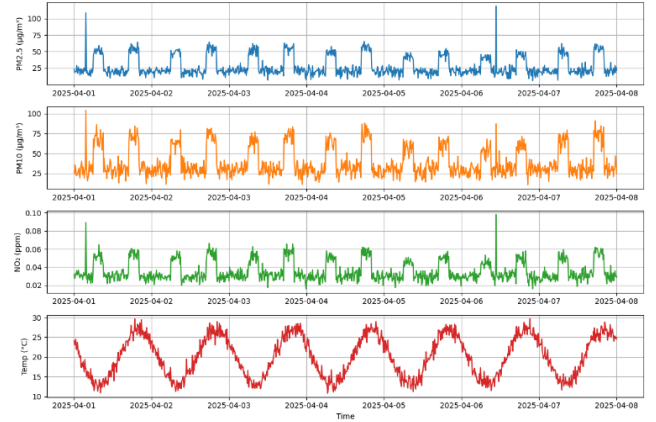


Fig. 11. Time-series variation of key air-quality parameters ($\text{PM}_{2.5}$, PM_{10} , NO_2) and meteorological variables collected from the CleanCity IoT mobile sensing system.

To further assess data richness and distributional characteristics, histogram plots for all pollutants and environmental variables are shown in Fig. 12. These distributions demonstrate substantial variability across measured concentrations, with PM_{10} and $PM_{2.5}$ showing multimodal behavior associated with alternating high-traffic and low-traffic conditions. Gaseous pollutants (NO_2 , SO_2 , O_3) present narrower distributions, typical of background urban air composition, while CO_2 ranges reflect both ambient outdoor levels and intermittent vehicle exhaust influence.

The completeness of the dataset was evaluated using the metric.

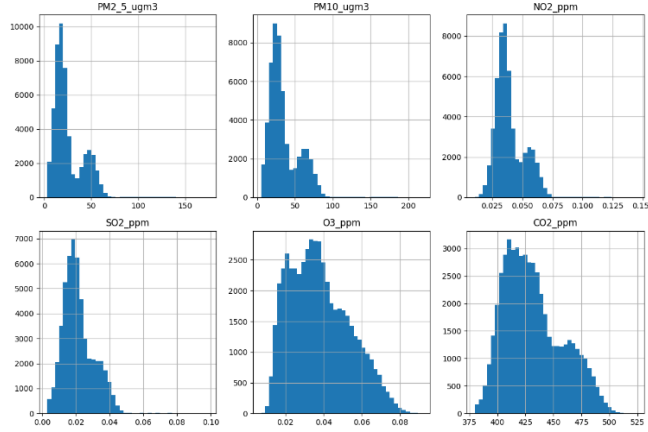


Fig. 12. Distribution of pollutant and environmental variables, illustrating concentration variability and underlying statistical patterns within the dataset.

where, N_s is the number of successfully uploaded samples and N_t is the expected number of samples based on the configured transmission interval. The system maintained high data availability across the monitoring period, confirming robust GSM connectivity and effective packet buffering in the LilyGO T-Call ESP32 board. Collectively, the time-series behavior, variable distributions, and high completeness rate validate the dataset as a reliable basis for subsequent LSTM-based forecasting and statistical analysis of urban air-quality dynamics.

B. System Performance Evaluation

The CleanCity IoT mobile sensing platform was deployed on a vehicle and evaluated under real urban operating conditions to assess communication stability, data reliability, environmental robustness, and cloud-integration performance. The LilyGO T-Call ESP32 board, equipped with the SIM800L GSM/GPRS module, demonstrated stable mobile connectivity throughout the monitoring period. The system achieved a high upload success rate, with most packets reaching the cloud on the first transmission attempt. Occasional GSM signal drops were mitigated by the built-in buffering mechanism, allowing queued packets to be retransmitted automatically once connectivity resumed.

The sensor suite also exhibited consistent and predictable behavior, as demonstrated by the correlation structure among the measured variables in Fig. 13. Strong positive correlations between $PM_{2.5}$ and PM_{10} confirm expected particulate co-variability in traffic-related environments, while moderate

relationships between gaseous pollutants reflect common emission sources along the vehicle routes. The negative correlation between temperature and humidity follows typical micro-meteorological conditions in Kigali's urban climate, further validating sensor stability.

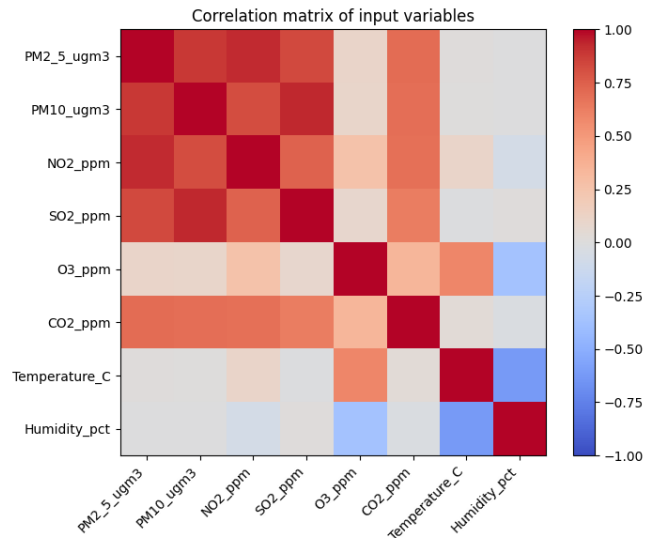


Fig. 13. Correlation matrix illustrating interdependencies between pollutant concentrations and meteorological variables

The data transmission latency averaged 2-4 seconds per packet during motion, consistent with typical GSM-based IoT deployments. The cloud dashboard updated in near real time, enabling effective monitoring of pollutant trends and environmental changes as the vehicle traversed different locations. Additionally, the hardware system demonstrated resilience to vibration, temperature changes, and power fluctuations during mobile operation. Overall, the system performance confirms that the CleanCity IoT platform is reliable for continuous mobile sensing in urban environments, maintaining stable communication, accurate sensing behavior, and real-time cloud integration suitable for further analytics and forecasting applications.

C. Machine Learning Model Performance

The cleaned and preprocessed multivariate dataset was used to train an LSTM-based forecasting model designed to predict short-term pollutant concentrations in real time. Input sequences were constructed using sliding windows of length L , where each window (Eq 16) represents the normalized and filtered sensor readings across all eight variables. The model produces a prediction (Eq 18) where f_θ denotes the LSTM, network parameterized by θ .

Model training converged smoothly, with the mean squared error (MSE) for both training and validation sets decreasing consistently, as shown in Fig. 14. The validation curve remained stable without divergence, indicating good generalization and absence of overfitting.

1) *Prediction accuracy on key pollutants:* The prediction performance for $PM_{2.5}$ and PM_{10} is shown in Fig. 15, where the predicted values closely follow the temporal structure of the true sensor measurements. The model successfully captures

peaks, transitions, and low-concentration periods, demonstrating strong short-term forecasting capability.

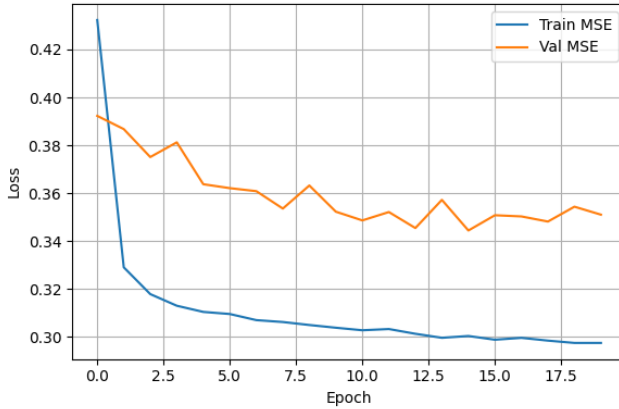


Fig. 14. Training and validation loss curves of the LSTM model, demonstrating convergence behavior and generalization performance.

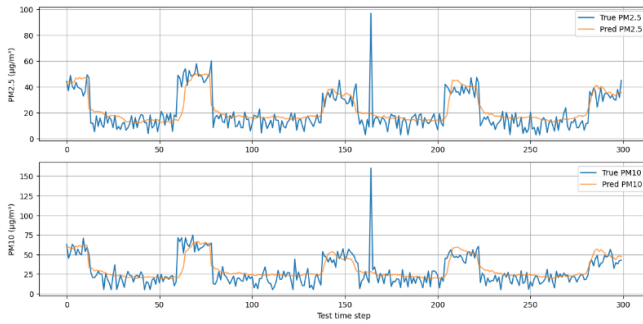


Fig. 15. Comparison between ground-truth and LSTM-predicted concentrations for PM_{2.5} and PM₁₀ over selected test windows.

2) *Model fit across all variables*: Scatter plots comparing predicted versus true values for all pollutants and environmental variables are shown in Fig. 16. The clustering of points around the 1:1 line demonstrates strong model agreement, especially for CO₂, temperature, O₃, and NO₂. Variability in PM_{2.5} and SO₂ predictions reflects the intrinsic noisiness of mobile-sensing particulate measurements.

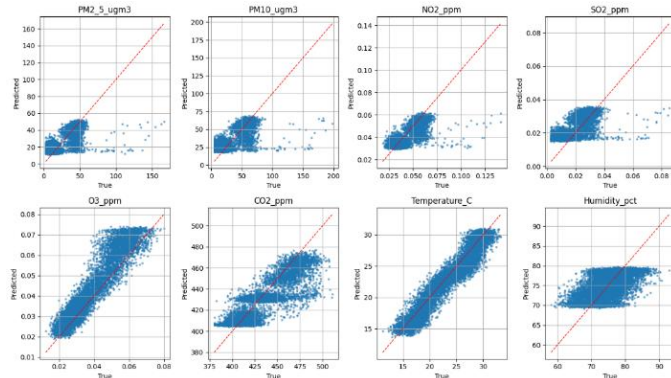


Fig. 16. Scatter plots comparing true and predicted values for all variables, with the 1:1 reference line indicating model accuracy.

3) *Error distribution*: To further examine predictive behavior, Fig. 17 presents the error distribution for PM_{2.5}. The

histogram shows a narrow, approximately Gaussian distribution centered close to zero, indicating low systematic bias and moderate variance in short-term particulate predictions.

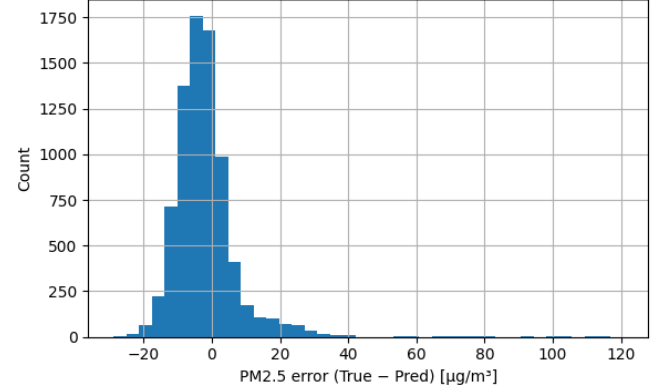


Fig. 17. Error distribution of PM_{2.5} predictions, highlighting bias and variance characteristics of the LSTM model.

4) *Quantitative metrics*: Summarizes the evaluation metrics for each variable, including MAE, RMSE, and MAPE. The LSTM model achieved strong predictive performance for temperature, CO₂, O₃, and NO₂, while PM_{2.5} and PM₁₀ exhibited higher relative errors due to their higher temporal variability and sensitivity to rapid environmental changes (Table III) during vehicle motion.

TABLE III. PERFORMANCE METRICS (MAE, RMSE, MAPE) OF THE LSTM MODEL ACROSS ALL POLLUTANTS AND ENVIRONMENTAL VARIABLES

Variable	MAE	RMSE	MAPE_percent
PM2_5_ugm3	6.83	10.45	61.41
PM10_ugm3	9.26	13.72	56.24
NO2_ppm	0.005	0.007	12.993
SO2_ppm	0.006	0.007	68.230
O3_ppm	0.005	0.006	14.537
CO2_ppm	10.64	14.39	2.42
Temperature_C	1.19	1.49	5.40
Humidity_pct	3.25	4.06	4.40

Overall, the LSTM model demonstrates strong capability in short-term pollutant forecasting across multiple variables. Stability in the loss curve, tight clustering in scatter plots, realistic error distributions, and favorable MAE/RMSE/MAPE scores confirm that the forecasting framework is effective for real-time deployment in mobile urban air-quality monitoring systems.

D. Assembled Edge Device with Deployed Model

The complete air-quality monitoring unit was integrated into a compact, weather-resistant enclosure and mounted on the front of a motorcycle to enable continuous mobile sensing across urban routes. As shown in Fig. 18, the device securely attaches to the motorcycle's suspension frame, ensuring minimal vibration interference while maintaining unobstructed airflow to

the sensing chamber. The embedded ESP32-SIM800L controller executes the trained machine-learning model directly on the edge, enabling on-device preprocessing, anomaly filtering, and real-time prediction without reliance on cloud-based computation.



Fig. 18. Clean city IoT device mounted on motorcycle.

The internal hardware layout, presented in Fig. 19, illustrates the modular arrangement of components including the PM and gas sensors, power system, GSM communication module, and microcontroller. The wiring architecture was optimized to reduce electromagnetic interference and to maintain sensor accuracy during mobile operation. This assembly design ensures robustness under typical road conditions while maintaining low power consumption, making it suitable for long-term vehicular deployments.

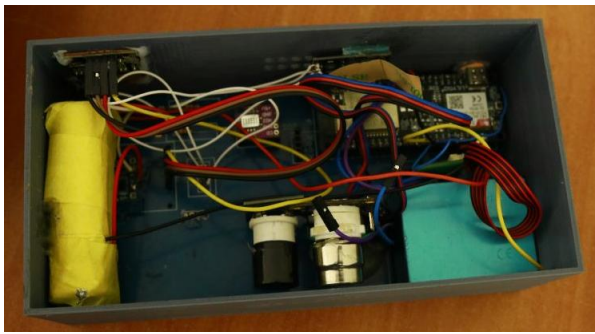


Fig. 19. Internal hardware layout of clean city IoT device.

E. Dashboard for Remote Monitoring

A web-based dashboard was developed to provide real-time visualization and remote access to sensor measurements, model inferences, and device status. The interface, shown in Fig. 20, displays pollutant concentrations (PM2.5, PM10, SO₂, NO₂, O₃, CO₂) alongside temperature and humidity, each represented with intuitive color codes and threshold indicators. This enables rapid

interpretation of air-quality conditions by operators and supports downstream analytics such as hotspot identification and route-based pollution profiling.

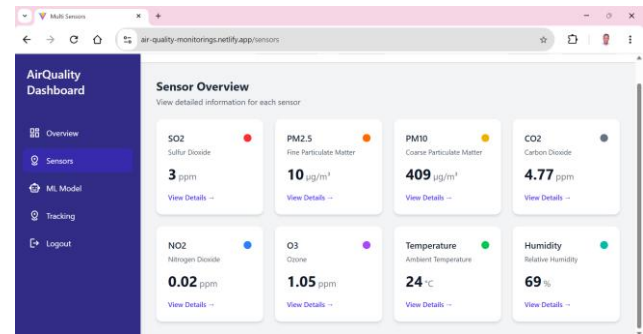


Fig. 20. Web-based remote monitoring dashboard of clean city IoT device.

The dashboard integrates seamlessly with the GSM-enabled edge devices via the cloud backend, allowing continuous updates at fixed intervals. Users may access detailed historical charts, inspect sensor-level readings, or monitor multiple devices simultaneously. This platform improves situational awareness and supports data-driven decision-making for urban air-quality management.

V. DISCUSSION

The results obtained from the mobile air-quality monitoring platform highlight the strong potential of integrating low-cost sensing, edge intelligence, and mobile data acquisition to provide high-resolution pollution insights in dynamic urban environments. The temporal plots and distribution analyses demonstrate that the system successfully captured realistic pollutant patterns, including recurring diurnal behaviors, peak concentrations along traffic corridors, and rapid fluctuations associated with vehicle-dense areas. These trends align with previously reported characteristics of mobile sensing platforms, reinforcing the reliability of the collected dataset.

The performance of the LSTM model reflects both the strengths and inherent challenges of forecasting air-quality parameters in mobile conditions. Temperature, humidity, CO₂, and O₃ predictions achieved low MAE and RMSE values, indicating that their temporal structures exhibit smoother and more predictable patterns that are well-suited to sequence-learning models. Conversely, higher error values observed for PM2.5 and PM10 are consistent with the behavior of particulate pollutants, which often vary sharply due to localized dust sources, abrupt vehicle acceleration, wind disturbances, or sudden micro-spikes near emission points. These high-frequency fluctuations pose a challenge for recurrent models, which assume gradual temporal transitions. Despite this, the predicted sequences still closely follow the underlying pollutant trends, suggesting that the LSTM architecture provides valuable short-term predictive capability.

The correlation matrix further reinforces the internal consistency of the dataset by revealing strong associations between combustion-related pollutants (PM2.5, PM10, NO₂, SO₂). These relationships are well documented in air-quality literature and confirm that the system effectively captured realistic vehicular emission profiles. The inclusion of

meteorological parameters in the model input contributed to performance stability by providing contextual information on atmospheric dispersion, temperature-dependent sensor responses, and humidity-driven particle behavior.

Operationally, the motorcycle-mounted sensing device (Fig. 18, Fig 20) validated the practicality of a low-power, mobile, GSM-enabled platform for real-time air-quality assessment. The device maintained stable measurements during movement and reliably transmitted data to the cloud dashboard. The remote monitoring interface (Fig. 20) enabled seamless visualization of pollutant levels, supporting quick interpretation and forming a foundation for future large-scale deployments. This capability is particularly valuable in resource-constrained environments where installing dense networks of fixed monitoring stations is not feasible.

Nonetheless, several limitations were observed. The elevated prediction errors for particulate matter indicate the need for more advanced filtering or hybrid modeling techniques such as Kalman filters, temporal attention mechanisms, or transformer-based architectures better suited for abrupt pollutant variability. Occasional GSM transmission delays highlight a trade-off between mobile connectivity and data continuity, suggesting that buffering strategies or 4G/LTE-based modules may be advantageous in future iterations. Sensor drift and long-term degradation pose additional challenges, underscoring the importance of periodic recalibration, redundancy, or sensor fusion approaches to maintain long-term reliability.

The findings demonstrate that mobile IoT sensing combined with edge-deployed machine-learning models provide a powerful and scalable approach to capturing granular air-quality information. It offers a practical pathway toward city-wide mobile pollution mapping, intelligent fleet monitoring, and data-driven environmental planning, especially in developing urban regions where cost-effective solutions are essential.

VI. CONCLUSION, RECOMMENDATIONS, AND FUTURE WORK

This study presented a mobile air-quality monitoring platform that integrates low-cost sensors, an ESP32-SIM800L edge device, GSM-based communication, and an LSTM prediction model to enable high-resolution pollution monitoring in dynamic urban environments. The mobile system successfully captured realistic temporal patterns of key pollutants including PM2.5, PM10, SO₂, NO₂, and O₃ while simultaneously collecting meteorological variables relevant to dispersion and atmospheric behavior. The experimental results demonstrated that the model accurately predicted smoother variables such as temperature, humidity, CO₂, and O₃, while exhibiting higher, yet consistent, errors for particulate matter due to its inherently abrupt and highly localized fluctuations. Overall, the system validated the feasibility of using a low-cost, edge-intelligent, mobile sensing approach to complement existing fixed monitoring infrastructures particularly in regions where traditional stations are sparse or economically prohibitive. The combination of real-time edge inference and cloud-based visualization provides a scalable foundation for city-wide monitoring, rapid hotspot identification, and informed environmental planning.

Model prediction errors for PM2.5 and PM10 highlight the need for more advanced temporal modeling techniques capable of handling sudden spikes and high-frequency variability. Network latency introduced by GSM connectivity suggests exploring more robust communication protocols and buffering strategies for uninterrupted data flow. Additionally, long-term reliability will require periodic sensor calibration, redundancy mechanisms, and drift-compensation strategies to maintain accuracy during extended deployments.

Based on these findings, the following recommendations are proposed:

- Adopt advanced hybrid modeling techniques: such as temporal attention mechanisms, transformer-based architectures, or Kalman-filter-enhanced LSTM to improve particulate matter forecasting.
- Upgrade communication infrastructure to LTE/4G or MQTT-based lightweight protocols to minimize transmission delays and enhance scalability.
- Implement periodic calibration schedules and sensor redundancy to mitigate drift, aging, and environmental contamination.
- Integrate geospatial and meteorological data sources (GIS layers, wind maps, road classifications) for more context-aware predictions and hotspot analysis.

Future work will focus on addressing these challenges by extending the system to support multi-node collaborative sensing, employing federated learning for distributed model updates, and exploring adaptive edge inference that dynamically adjusts sampling rates depending on environmental conditions. Additional work will investigate long-term deployment performance, data fusion with satellite products, and integration with policy tools for real-time air-quality alerts.

In conclusion, this research provides a practical, scalable, and cost-effective framework for mobile air-quality monitoring in rapidly urbanizing regions. By combining IoT sensing, edge computing, and machine learning, the system offers a promising direction for enhancing environmental intelligence and supporting evidence-based public health interventions.

ACKNOWLEDGMENT

The team acknowledges the support of the University of Rwanda, College of Science and Technology, and its African Centre of Excellence in Internet of Things (ACEIoT) for the use of their facilities and laboratory.

REFERENCES

- [1] S. A. Siddiqui, N. Fatima, and A. Ahmad, "Smart Air Pollution Monitoring System with Smog Prediction Model using Machine Learning," *Int. J. Adv. Comput. Sci. Appl.*, vol. 12, no. 8, pp. 401–409, 2021, doi: 10.14569/IJACSA.2021.0120846.
- [2] E. R. I. Mogo, A. Lemo, C. Abdeta, and O. Olufemi, "Mounting an effective socio-ecological response to non-communicable diseases in Africa's cities," *Cities Heal.*, vol. 6, no. 1, pp. 51–56, 2022, doi: 10.1080/23748834.2019.1688911.
- [3] G. Rincon, G. Morantes, A. Garcia-Angulo, S. Mota, M. del P. Cornejo-Rodriguez, and B. Jones, "Understanding particulate matter emissions from cooking meals, health impacts and policy path in Ecuador," *Sci.*

Total Environ., vol. 982, p. 179628, Jun. 2025, doi: 10.1016/J.SCITOTENV.2025.179628.

[4] R. Subramanian et al., "Research article Air pollution in Kigali, Rwanda: spatial and temporal variability, source contributions, and the impact of car-free Sundays," Clean Air J., vol. 30, no. 2, pp. 1–15, 2020, doi: 10.17159/CAJ/2020/30/2.8023.

[5] D. Zboralski and M. Kunz, "Mobile systems for assessing air quality: available solutions and application examples," Bull. Geogr. Phys. Geogr. Ser., vol. 27, no. 27, pp. 5–26, 2024, doi: 10.12775/bgeo-2024-0007.

[6] C. Correia et al., "A Low-Cost Sensor System Installed in Buses to Monitor Air Quality in Cities," Int. J. Environ. Res. Public Health, vol. 20, no. 5, 2023, doi: 10.3390/ijerph20054073.

[7] B. Zherka and Z. Tafa, "A Vehicle Sensor Network for Real-Time Air Pollution Analysis," J. Adv. Inf. Technol., vol. 14, no. 1, pp. 39–45, 2023, doi: 10.12720/jait.14.1.39-45.

[8] P. Santana, A. Almeida, P. Mariano, C. Correia, V. Martins, and S. M. Almeida, "Air quality mapping and visualisation: An affordable solution based on a vehicle-mounted sensor network," J. Clean. Prod., vol. 315, p. 128194, Sep. 2021, doi: 10.1016/J.JCLEPRO.2021.128194.

[9] K. Ivanova, T. Branzov, and N. Ivanova, "IoT on the roofs of municipally governed vehicles for air pollution tracking," CEUR Workshop Proc., vol. 2803, pp. 172–177, 2020.

[10] Nizeyimana, Eric, Hwang, Junseok, Zirikana, Jules, Karikumutima, Bonaventure, Mihigo, Irene Niyonambaza, Nizeyimana, Pacifique, Hanyurwimfura, Damien, Nsenga, "Revolutionizing Air Pollution Spikes Analysis With a Blockchain - Driven Machine Learning Framework," Trans. Emerg. Telecommun. Technol., vol. 36, no. 5, 2025, doi: 10.1002/ett.70143.

[11] E. Nizeyimana, J. Nsenga, R. Shibasaki, D. Hanyurwimfura, and J. Hwang, "Design of Smart IoT Device for Monitoring Short-term Exposure to Air Pollution Peaks," Int. J. Adv. Comput. Sci. Appl., vol. 13, no. 1, 2022, doi: 10.14569/IJACSA.2022.0130103.

[12] P. Santana, A. Almeida, P. Mariano, C. Correia, V. Martins, and S. M. Almeida, "Air quality mapping and visualisation: An affordable solution based on a vehicle-mounted sensor network," J. Clean. Prod., vol. 315, no. July, 2021, doi: 10.1016/j.jclepro.2021.128194.

[13] P. Bansal, "Charging of electric vehicles: Technology and policy implications," J. Sci. Policy Gov., vol. 6, no. 1, pp. 1–20, 2015.

[14] V. Devasekhar and P. Natarajan, "Prediction of Air Quality and Pollution using Statistical Methods and Machine Learning Techniques," Int. J. Adv. Comput. Sci. Appl., vol. 14, no. 4, pp. 927–937, 2023, doi: 10.14569/IJACSA.2023.01404103.

[15] H. S. Russell, L. B. Frederickson, M. O. B. Sørensen, J. A. Schmidt, O. Hertel, and M. S. Johnson, "Hyperlocal Air Pollution in London: Validating Low-Cost Sensors for Mobile Measurements from Vehicles," ACS ES&T Air, vol. 1, no. 6, pp. 438–450, 2024, doi: 10.1021/acsestair.3c00043.

[16] S. Saleh, A. S. Abohamama, and A. S. Tolba, "Intelligent Real-Time Air Quality Index Classification for Smart Home Digital Twins," Int. J. Adv. Comput. Sci. Appl., vol. 16, no. 3, pp. 309–323, 2025, doi: 10.14569/IJACSA.2025.0160331.

[17] A. H. M. Shaberi, S. Dzulkifly, W. S. Li, and Y. F. A. Gaus, "Machine Learning Approaches for Predicting Occupancy Patterns and its Influence on Indoor Air Quality in Office Environments," Int. J. Adv. Comput. Sci. Appl., vol. 15, no. 9, pp. 853–860, 2024, doi: 10.14569/IJACSA.2024.0150987.

[18] A. A. Aserkar, S. R. Godla, Y. A. Baker El-Ebiary, Krishnamoorthy, and J. V. N. Ramesh, "Real-time Air Quality Monitoring in Smart Cities using IoT-enabled Advanced Optical Sensors," Int. J. Adv. Comput. Sci. Appl., vol. 15, no. 4, pp. 840–848, 2024, doi: 10.14569/IJACSA.2024.0150487.

[19] Y. Wang, R. Sun, Q. Cheng, and W. Y. Ochieng, "Measurement Quality Control Aided Multisensor System for Improved Vehicle Navigation in Urban Areas," IEEE Trans. Ind. Electron., vol. 71, no. 6, pp. 6407–6417, 2024, doi: 10.1109/TIE.2023.3288188.

[20] Q. Zhang, Y. Han, V. O. K. Li, and J. C. K. Lam, "Deep-AIR: A Hybrid CNN-LSTM Framework for Fine-Grained Air Pollution Estimation and Forecast in Metropolitan Cities," IEEE Access, vol. 10, pp. 55818–55841, 2022, doi: 10.1109/ACCESS.2022.3174853.